RDU090364

DEVELOPMENTS OF ANEURYSM RUPTURE PREDICTION METHOD USING FRACTURE MECHANICS ANALYSIS

(PEMBANGUNAN KAEDAH JANGKAAN PEMECAHAN ANEURISMA MENGGUNAKAN ANALISIS MEKANIK REKAHAN)

JULIAWATI BINTI ALIAS
MOHAMAD MAZWAN MAHAT
MOHD AKRAMIN MOHD ROMLAY

RESEARCH VOTE NO:
RDU090364

Fakulti Kejuruteraan Mekanikal
Universiti Malaysia Pahang

2010

ACKNOWLEDGEMENT

Alhamdulillah, thanks to Allah the almighty for his blessing to complete the research by the given duration. Thanks to all the people who have contributed and sincerely worked on this research.

ABSTRACT

NUMERICAL MODELING OF ANEURYSM GROWTH AND RUPTURE

(Keywords: Aneurysm, Numerical method, Fluid structure interaction)

This study attempted to investigate the aneurysms growth and rupture using numerical approach. The bulging and widening of the blood vessel is due to the weakening of its wall which may lead the patient to death if rupture point is reached. This phenomena occur due to blood dynamics parameters which driven under certain flow conditions. It also has a tendency to enlarge over the years, depending on several factors. In order to obtain the deformation profiles, the fluid structure interaction method (FSI) was utilized to obtain the wall conditions of aneurysm ruptured. In addition, the numerical modelling of aneurysms results the blood flow parameter of pressure and velocity inside aneurysm sac in the form of profile correlations. The FSI transferred these dynamics loads to exert the aneurysms wall to determine the respective deformations. It is expected to explain the effect of blood flow to the weakening vessel wall and rupture behaviour due to variable flow conditions. These results assist medical practitioner to the prediction of time and location of aneurysm ruptured.

Key researchers :

M.Mazwan Mahat

A. Juliawati

M.R.M. Akramin

E-mail : ***(juliawati@ump.edu.my)***

Tel. No. : 013-7791902

Vote No. : RDU090364

ABSTRAK

Kajian ini merupakan usaha untuk mengkaji pertumbuhan dan pemecahan aneurisma menggunakan pendekatan berangka. Pembengkakan dan peluasan saluran darah adalah disebabkan oleh kelemahan dindingnya yang boleh mengakibatkan pesakit mati jika titik pemecahan dicapai. Fenomena ini berlaku akibat parameter dinamik darah yang bergerak di bawah keadaan aliran yang tertentu. Ia juga mempunyai kecenderungan untuk membesar sepanjang tahun, bergantung kepada beberapa faktor. Untuk mencapai profil perubahan bentuk, kaedah interaksi struktur cecair telah digunakan untuk memperolehi keadaan dinding aneurisma yang pecah. Model berangka aneurisma juga menunjukkan tekanan dan kelajuan di dalam kandungan aneurisma sebagai parameter aliran darah dalam bentuk korelasi profil. Kaedah interaksi struktur cecair telah memindahkan beban dinamik tersebut yang digunakan pada dinding aneurisma bagi menentukan perubahan bentuk tersebut. Keputusan kajian menjangkakan, kesan aliran darah terhadap dinding saluran darah yang lemah dan kelakuan pemecahan disebabkan keadaan aliran pembolehubah. Keputusan membantu pengamal perubatan untuk jangkaan masa dan lokasi pemecahan aneurisma.

TABLE OF CONTENTS

LIST OF TABLE

LIST OF FIGURE

LIST OF SYMBOL/ ABBREVIATIONS

AAA	Abdominal Aortic Aneurysm
CFD	Computational Fluid Dynamic
CT	Computed Tomography
EFD	Engineering Fluid Dynamic
EVAR	Endovascular Aneurysm Repair
FSI	Fluid Structure Interaction
ILT	Intraluminal Thrombus

CHAPTER 1

Introduction

The numerical method is applied to model blood flow in aneurysms to study the effect of stenting to the growth rate of aneurysms. The objective of this study is to develop numerical models to analyze the wall deformation due to various type of stent. Computational Fluid Dynamics is known as a powerful alternative approach in solving various fluid flow phenomena. This provides us the opportunity for to go deeper into the blood flow and understand how the interaction between them would affect the macroscopic parameters of blood flow.

Aneurysm is a degenerative disease which abnormality appears in the form of dilation of a blood vessel due to weakening of its wall. The vessel may rupture and cause life threatening bleeding if not surgically treated. Currently, two methods are available for treatment of aneurysm – open surgery or endovascular aneurysm repair. The first treatment uses synthetic polymeric graft to replace the diseased site, whilst the second involves strengthening the blood vessel wall with an expandable metallic stent. Endovascular aneurysm repair is gaining popularity over open surgery, but the technique is relatively new without long-term follow-up outcome. Pre-clinical evaluations are therefore crucial to minimise possible complications such as endoleaks, stent migration, stent failure and other complications. The analysis of stented aneurysms model using numerical methods to study the interactions between the stent and the blood vessel wall have been conducted both in two and three dimensions [1, 2, 3, and 4]. These studies investigate among other things the stresses and strains exerted on the blood vessel wall, strut strength of the stent, and the degree of stent flexibility. Predictions from finite element analyses confirmed the altered haemodynamics of stented vessel found experimentally and actual complications found after surgery.

Generally, there are two shapes of aneurysms; fusiform and saccular. The existing treatment procedures do not provide suitability for fusiform aneurysms [5] and therefore, stenting becomes an experimental alternative for these aneurysms. Many successful clinical cases have been reported [5,6] due to stent implantation that works effectively. Currently, few studies focused on stenting of fusiform aneurysms compared to saccular aneurysms in from of experimental and theoretical studies [5].

In surgical treatment, a stent graft is guided to the affected area of the blood vessel and then expanded by ballooning to create a new sleeve through which the blood can flow. The new sleeve will protect the weak wall of the blood vessel from the pulsatile blood pressure that could lead to rupture [7]. The technique has shown significant success for the treatment

of aneurysm, however, many post-operative complications such as stent migration, stent failure, and blood leakage may still occur. The metallic stent is normally made of surgical grade balloon expandable 316L stainless steel mesh tubes with diameter ranging from 2-4mm and length ranging from 8-38mm [2]. The open mesh comes in various configurations with two of the most common designs are the diamond-shape [1] and the tubular rings with bridging links [2]. Once introduced at the aneurysm site, the stent is expanded by inflating an angioplasty balloon with an inflating pressure between 12 to 18 atmospheres [3]. The stent will eventually fuse with the blood vessel wall with tissue ingrowths surrounds the open mesh.

The changes of local velocity and pressure inside the aneurysm lead to vortex formation and complex flow structure exist in blood vessel around the aneurysm. These phenomena become a common finding from previous numerical study. The fluid phenomena found by previous work revealed almost similar flow pattern. The vortex formation could be explained due to the pressure imbalance that leads to the swirl in aneurysm. But, the strength of the swirl is not yet investigates by any researcher to relate with either the size of aneurysm or specific location of detected diseased.

Problem Statement

Aneurysm is a degenerative disease which abnormality appears in the form of dilation of a blood vessel due to weakening of its wall. The vessel may rupture and cause life threatening bleeding if not surgically treated. Method to predict the rupture point and time is very crucial to avoid sudden death.

This research utilize numerical method to develop the newly method of aneurysms rupture prediction.

Research Objectives

i. To develop the newly rupture prediction technique
ii. To determine the fracture characteristics in terms of rupture point and time of aneurysms.

CHAPTER 2

1st TECHNICAL PAPER PUBLISHED

EnCon2010, 3rd Engineering Conference on Advancement in Mechanical and Manufacturing for Sustainable Environment, April 14-16, 2010, Kuching, Sarawak, Malaysia

Proceedings of EnCon2010
3rd Engineering Conference on Advancement
in Mechanical and Manufacturing for Sustainable Environment
April 14-16, 2010, Kuching, Sarawak, Malaysia

Numerical Modeling of Aneurysm Growth and Rupture

M.Mazwan Mahat, A. Juliawati and M.R.M. Akramin

Abstract— **This study attempted to investigate the aneurysms growth and rupture using numerical approach. The bulging and widening of the blood vessel is due to the weakening of its wall which may lead the patient to death if rupture point is reached. This phenomena occur due to blood dynamics parameters which driven under certain flow conditions. It also has a tendency to enlarge over the years, depending on several factors. In order to obtain the deformation profiles, the fluid structure interaction method (FSI) was utilized to obtain the wall conditions of aneurysm ruptured. In addition, the numerical modelling of aneurysms results the blood flow parameter of pressure and velocity inside aneurysm sac in the form of profile correlations. The FSI transferred these dynamics loads to exert the aneurysms wall to determine the respective deformations. It is expected to explain the effect of blood flow to the weakening vessel wall and rupture behaviour due to variable flow conditions. These results assist medical practitioner to the prediction of time and location of aneurysm ruptured.**

Keywords: Aneurysm, Numerical method, Fluid structure interaction.

I. INTRODUCTION

Aneurysm is a growing dilation of non-reversible blood flow due the weakening of blood vessel which may lead to rupture if not further treated [1]. In modern approach, there are two treatments available; aneurysm-open surgery and endovascular aneurysm repair (EVAR). In EVAR, the guided stent being inserted at the diseased blood vessel and then inflated by ballooning catheter to create a new sleeve which may mechanically protect the weakening of the wall from the pulsate blood pressure that brought to high rupture risk [1,2]. Generally, there are two shapes of aneurysms; fusiform and saccular. The existing treatment procedures do not provide suitability for fusiform aneurysms [3] and therefore, stenting becomes an experimental alternative for these aneurysms. Many successful clinical cases have been reported [4,5] due to stent implantation that works effectively.

This work was supported by UMP as provider of solver and whole processing tools of modeling activities.

M.Mazwan Mahat was previously with UMP and he is now with the Faculty Of Mechanical Engineering, Universiti Teknologi MARA(UiTM) Shah Alam, 40450 Shah Alam, Selangor. Phone: 603-5543 6248; (e-mail: mazwan@salam.uitm.edu.my).

A.Juliawati, is with the Faculty Of Mechanical Engineering, Universiti Malaysia Pahang, Lebuhraya Tun Razak, 26300 Gambang, Kuantan, Pahang (e-mail: juliawati@ump.edu.my). She is the leader for RDU090364 grant.

M.R.M. Akramin is with the Faculty Of Mechanical Engineering, Universiti Malaysia Pahang, Lebuhraya Tun Razak, 26300 Gambang, Kuantan, Pahang (e-mail: akramin@ump.edu.my).

The changes of local velocity and pressure inside the aneurysm lead to vortex formation and complex flow structure exist in blood vessel around the aneurysm. These phenomena become a common finding from previous numerical research. The vortex formation could be explained due to the pressure imbalance that leads to the swirl in aneurysm. But, the strength of the swirl is not yet investigates by any researcher to relate with either the size of aneurysm or specific location of detected diseased.

The investigation towards detection of aneurysm rupture, consideration should focus on both of non-geometric patient characteristic and geometric properties [6]. In recent study, computational model of mechanical behaviour in an aneurysm is most prominent trend in an aneurysm rupture risk assessment through the improvement of imaging and segmentation [10]. Study on idealised geometries model shown the wall stress is significantly reduced in presence of intraluminal thrombus (ILT) but the size of aneurysm and constitutive properties of aortic wall is considered [8]. In addition, the effect of aneurysm wall was increasing due the presence of atherosclerotic plaques inside blood vessel [8]. On the other hand, the stress distribution was depended on the real aneurysm shapes as well as the maximum diameter [7]. In actual geometrical shape of aneurysms, there is a highly complex of an aneurysm in vivo shape and far from axisymmetric [12], which specific wall stress assessment and finite element models were the mainly approach need to be based on detailed for an aneurysm geometry of those three dimensional description. The complex wall stress distribution was shown from the modeled based on patient-specific geometries [9], which may influence after the presence of ILT [10]. Furthermore, there has been related between the occurrence and location [11] of aneurysm rupture and the peak wall stress value that computed from this aneurysm model. From the observation, the peak wall stress was a better predictor of aneurysm rupture than diameter in an aneurysm [9]. The boundary condition for the pressure load was applied at the vessel wall which is resulted from the coupled of blood velocity and pressure.

II. NUMERICAL MODELING

In general, computational fluid dynamic (CFD) techniques have the advantage of a greater flexibility with respect to the experimental or *in vivo* methods [17]. For the CFD simulations carried out in this study, it is assumed that blood is an incompressible, Newtonian fluid and that the flow is laminar and isothermal. Blood exhibits non-Newtonian behaviors [18]. However, in many cases for large enough vessels and fast enough flows, a Newtonian approximation is sufficient. However it still depend on the situation, which blood behaves as a non-Newtonian fluid when shear rate increases, the blood viscosity decreases. But, this feature is prominent for small arteries, whereas Newtonian features are characteristic for large arteries. Therefore, there is no significant difference for Newtonian and non-Newtonian flow within an aneurysm, which was confirmed in [18] and others who found minimal changes in arterial flow patterns when non-Newtonian effects were included. Thus, the Newtonian blood model was assumed in this study.

Since arteries are viscoelastic structure, the interactions between artery walls and blood cause that endothelial cells are under continuous pressure. Measurement of artery wall properties may be very hard task as properties of healthy and diseased vessels are varied. On the other hand, healthy arteries are highly deformable complex structures, characterized by a nonlinear strain–stress curve with exponential rigidity in the higher strain ranges. This rigidity effect, characteristic for all biological tissues, is the result of rough collagen fibers which show typical anisotropic behavior [19]. From previous study, rigid walls were assumed for purpose of their study [14, 15, and 16] and this project will utilize the basic deformation theory to produce wall conditions. Other parameters such as density, dynamic viscosity,

thermal conductivity and specific heat are according to normal blood flow conditions. These values were assumed to be constant along the blood vessels during the simulations.

The physical laws describing the problem investigated here are the conservation of mass and the conservation of momentum. For such a fluid, the continuity and Navier–Stokes equations are as follows:

$$\frac{\partial u_i}{\partial x_i} = 0 \tag{1}$$

$$\rho\left(\frac{\partial u_i}{\partial t} + u_j\frac{\partial u_i}{\partial x_j}\right) = -\frac{\partial P}{\partial x_j} + \mu\frac{\partial^2 u_i}{\partial x_j \partial x_j} + f_i \tag{2}$$

Where u_i= velocity in the i^{th} direction, P = Pressure, f_i = Body force, ρ =Density, μ_i =Viscosity and ∂_{ij} = Kronecker delta. The shear stress, τ at the wall of aneurysm calculated base on a function of velocity gradient only:

$$\tau = \mu\frac{\partial u}{\partial y} \tag{3}$$

Where $\partial u/\partial y$ is the velocity gradient along the aneurismal wall taking considerations of fluid viscosity. Therefore, the simple viscous fluids considered with linear relationship. The equation of motion in terms of vorticity, ω as follows:

$$\frac{\partial \omega}{\partial t} - \nabla X (V X \omega) = \frac{\mu}{\rho}\nabla^2\omega \tag{4}$$

Where ω is the vorticity, ρ =Density and μ= viscosity with vector $\nabla^2 V$ evaluated as well.
In the frame of the ***k-ε*** turbulence model, μ_t is defined using two basic turbulence properties, namely, the turbulent kinetic energy ***k*** and the turbulent dissipation ε,

$$\mu_t = f_\mu\frac{C_\mu \rho k^2}{\epsilon} \tag{5}$$

Here, f_μ is a turbulent viscosity factor. It is defined by the expression

$$f_\mu = \left[1 - exp(-0.025R_y)\right]^2.\left(1 + \frac{20.5}{R_T}\right) \tag{6}$$

Where,

$$R_T = \frac{\rho k^2}{\mu_l \varepsilon}, R_y = \frac{\rho\sqrt{ky}}{\mu_l} \tag{7}$$

and y is the distance from the wall. This function allows us to take into account laminar-turbulent transition.

Two additional transport equations are used to describe the turbulent kinetic energy and dissipation,

$$\frac{\partial \rho k}{\partial t} + \frac{\partial}{\partial x_k}(\rho u_k k) = \frac{\partial}{\partial x_k}\left(\left(\mu_l + \frac{\mu_t}{\sigma_k}\right)\frac{\partial k}{\partial x_k}\right) + \mathcal{S}_k \tag{8}$$

$$\frac{\partial \rho \varepsilon}{\partial t} + \frac{\partial}{\partial x_k}(\rho u_k \mathcal{E}) = \frac{\partial}{\partial x_k}\left(\left(\mu_l + \frac{\mu_t}{\sigma_\varepsilon}\right)\frac{\partial \varepsilon}{\partial x_k}\right) + \mathcal{S}_\varepsilon \tag{9}$$

Here P_B represents the turbulent generation due to buoyancy forces and can be written as

$$P_B = -\frac{g_i}{\sigma_B}\frac{1}{\rho}\frac{\partial \rho}{\partial x_i} \tag{10}$$

where g_i is the component of gravitational acceleration in direction x_i, the constant σ_B= 0.9, and constant is defined as: C_B = 1when , and C_B = 0 otherwise;

$$f1 = 1 + \left(\frac{0.05}{f_\mu}\right)^3, f2 = 1 - exp(-R_T^2) \quad (11)$$

The constants Cμ, Cε1, Cε2 ,σk , σε are defined empirically. In that software, the following typical values are used:

$$C_\mu = 0.09, C_{\varepsilon l} = 1.44, C_{\varepsilon 2} = 1.92, \sigma_\varepsilon = 1.3$$
$$\sigma_k = 1$$

These equations describe both laminar and turbulent flows. Moreover, transitions from one case to another and back are possible. The parameters k and μ_t are zero for purely laminar flows.

Solution of these equations in their finite volume form is accomplished through a commercial software package Cosmoflow. The solver solves the governing equations with the finite volume (FV) method on a spatially rectangular computational mesh designed in the Cartesian coordinate system with the planes orthogonal to its axes and refined locally at the solid and fluid interface. Additional refining was done for specified blood regions, at the arterial and aneurysm surfaces during calculation. Values of all the physical variables are stored at the mesh cell centers and due to the Finite Volume method, the governing equations are discretized in a conservative form and the spatial derivatives are approximated with implicit difference operators of second-order accuracy. The time derivatives are approximated with an implicit first-order Euler scheme. The geometric dimensions of the side-wall aneurysm, the parent artery harboring the aneurysm were modeled using CAD commercial software.

III. RESULTS AND DISCUSSIONS

Velocity contour for the blood flow shows in figure 1 and figure 2 is the interaction between blood flow and the aneurysm wall. When the initial velocity of the blood flow increase about 0.1m/s, the flow pattern are change accordingly as the load follows the pulsation time. The highest velocity is 0.759m/s in the normal blood vessel with the inlet velocity,V_{inlet} = 0.7m/s in the 7mm diameter of blood vessel. The lowest velocity is 0.136m/s which the values came from the inlet velocity,V_{inlet} = 0.3ms with the same diameter of blood vessel.

The highest velocity in the abnormal blood vessel which have aneurysm at the arterial is 0.7715m/s with the inlet velocity,V_{inlet} = 0.7m/s. This happen because lack of blood velocity which going through the aneurysm. This mean, the aneurysm make an effect in the velocity of blood in the blood vessel and this will increase of pressure in the blood vessel.

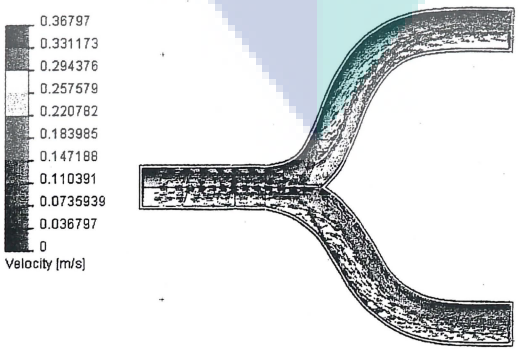

Figure 1: Velocity distribution for normal blood vessel

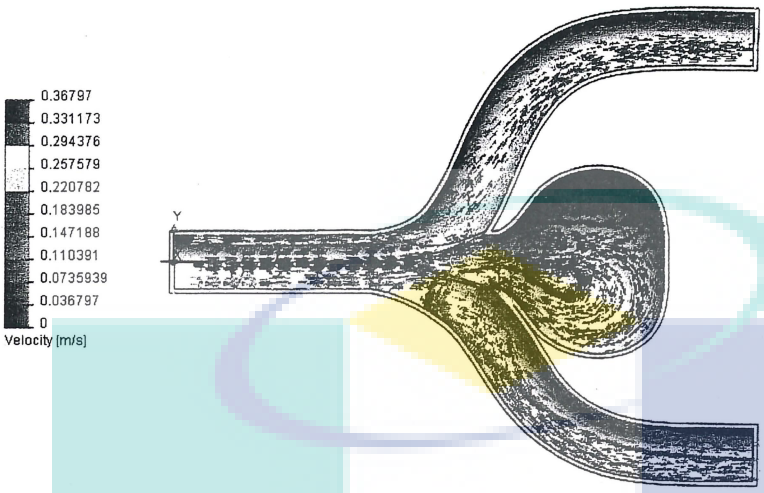

Figure 2: Velocity distributions for abnormal blood vessel (with aneurysm)

Base on both figures 1 and 2, the velocity of blood flow decreasing after hit the wall at the branch of blood vessel. Then, when the blood touched the wall at branches, the other particles of blood will flow separately. The simulation shows that less flow of blood particles at the upper wall of blood vessel.

Figure 3 and 4 below shows the result for changes of velocity in same diameter of blood vessel which is 7mm. Velocity blood flow changes increase about 0.1m/s for each analysis.

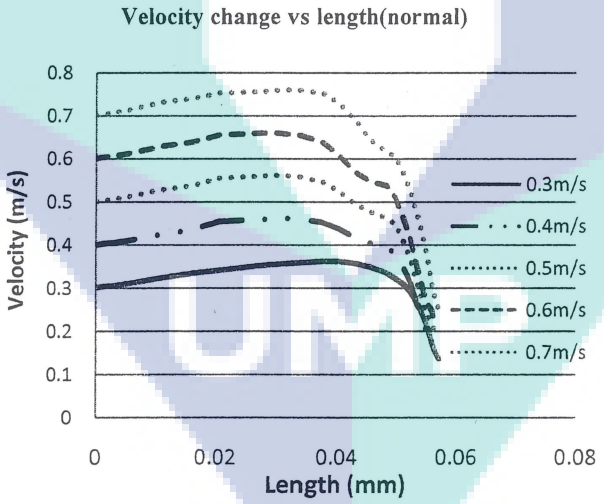

Figure 3: Graph velocity vs length for different velocity in normal case

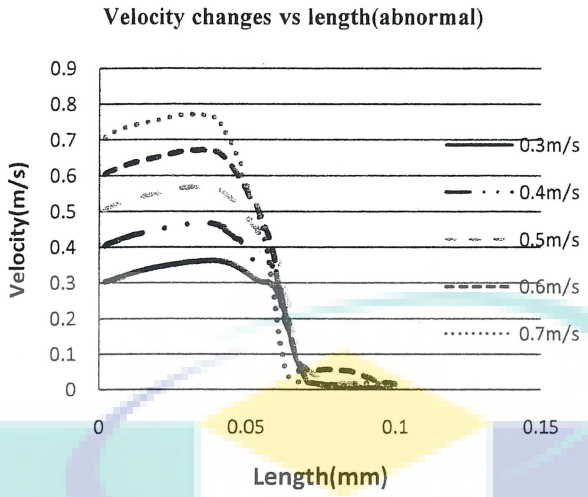

Figure 4: Graph velocity vs length for different velocity in abnormal case

We found that the result from analysis in different velocity for same diameter, agreed to energy conservation principles. Inlet velocity, V_{inlet} started at 0.3m/s until 0.7m/s have been attached to the entire model in boundary condition for simulation. Then, all the static pressure was set to the same value which is equal to 463 kPa. The increment of velocity was about 0.1m/s and the result show from the figure 3 and 4. For normal blood vessel, the velocity smoothly decrease and have slightly effected by the bifurcation. There was a few different for abnormal case. Aneurysm at the bifurcation gives a large impact to the velocity blood flow. The velocity decreases once the whole conduit of fluid transfer the energy in form of pressure.

Effects of blood vessel diameter

Figure 5 and 6 below shows simulation result for normal and abnormal blood vessel at one velocity inlet, 0.3 m/s. We model the aneurysm with variable diameter of blood vessel and the effect shown in the graph.

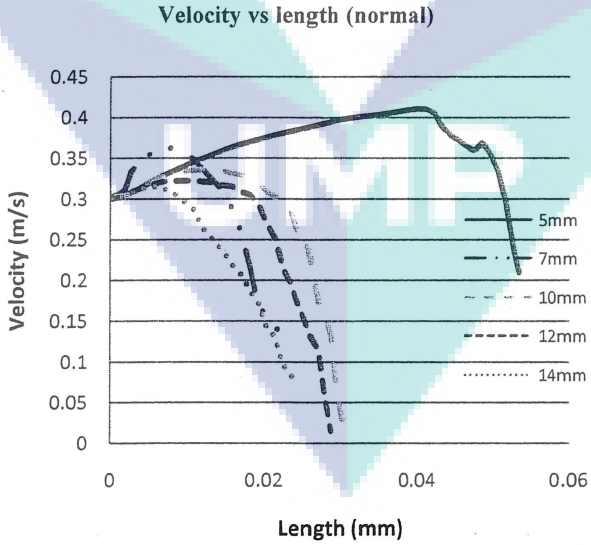

Figure 5: Graph velocity vs length for different diameter in normal case

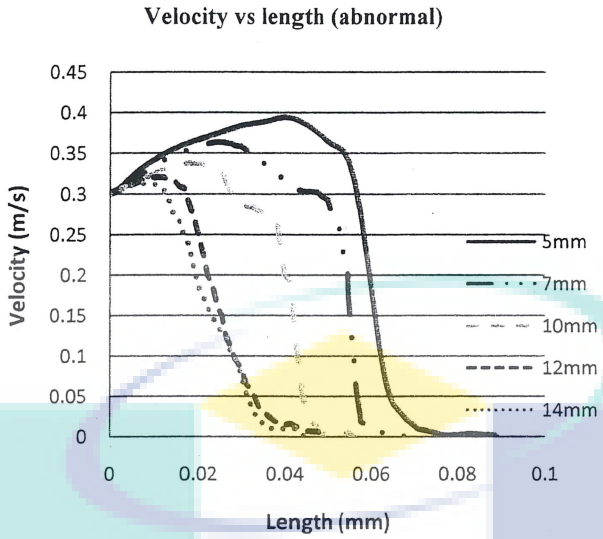

Figure 6: Graph velocity vs length for different diameter in abnormal case

In the figures above, the profile plot represent the velocity for two cases which are normal and abnormal case with different diameter construction. Both cases above had shown the effect of diameter in making the velocity of blood going more smoothly when it becomes bigger in size of diameter. These analysis also noted that the bifurcation give an effect to the result of blood parameter. For normal case, the velocity of blood flow when the diameter is 5mm higher than those having bigger diameter of blood vessel. It also happens for abnormal case with aneurysm. This means the velocity of blood going smoothly through the small diameter of blood vessel rather than the bigger size of diameter. Diameter of blood vessel gives an influence to the blood flow at the bifurcation.

Peak Velocity relations with vessel diameter

All the simulation figures shows below are the data for the variable diameter of blood vessel. Blood flow behavior shows a different pattern when the diameter of blood vessel increases. Peak velocity also considered in this analysis to know the effect of diameter changes in the aneurysm sac. The figure 7 and 8 below shows the comparison between the normal and abnormal blood vessel peak velocity vs diameter.

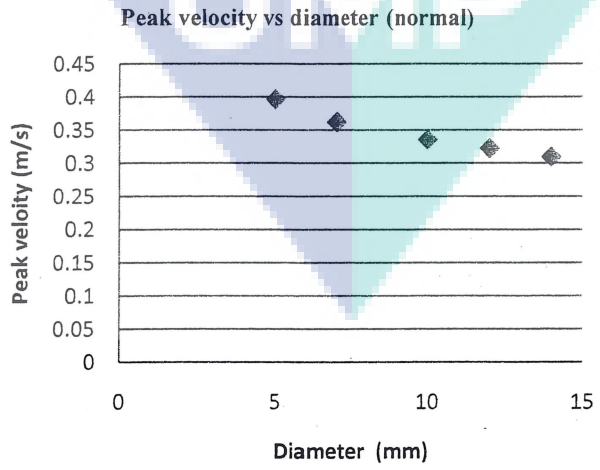

Figure 7: Peak velocity vs diameter for normal case

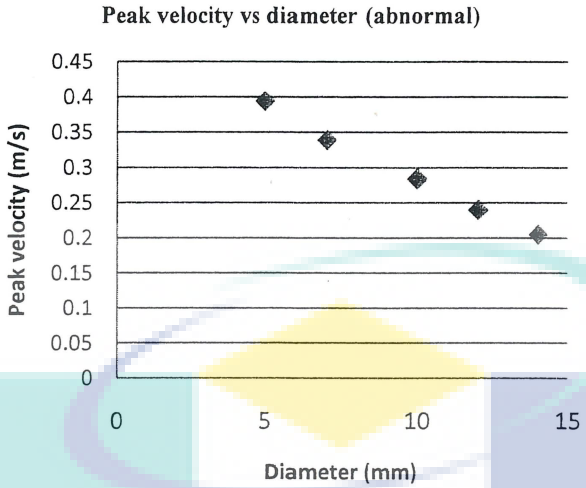

Figure 8: Peak velocity vs diameter for abnormal case

From the figure above,the different peak velocity percentage will get a bigger margin when it comes bigger diameter.The different peak velocity percentage for 5mm only about 0.61% and for 7mm it is about 6.4%.The normal case and abnormal case shown the different in peak velocity when the blood going throught the aneurysm and without aneurysm.The velocity of the blood will decrease when it comes into the aneurysm.It means,the aneurysm at the branches of the microvessel bifurcations give an effect to the blood flow behaviour.

The different percentage for 10mm,12mm and 14mm diameter of blood vessel also can be the proved that the velocity of the blood will decrease after the aneurysm.These will lead to the changes of behaviour of the blood flow and affect the blood vessel.

Flow Pattern of unruptured aneurysm

There are 3 stages of aneurysm deformation shows in a curvature. This section present the flow pattern in blood vessel through the modelling of the actual expanded that had been designed in three dimensions. The vortex formation increase the rate of aneurysm ruptured. The recirculation flow and vortex deformation near the aneurysm wall would produce the oscillatory curvature along the aneurysm region. The pattern was validated using Khanafer [20] model curvature which shows a similar pattern with the present study. The entire flow pattern from this study shows in figure 9 to 11 for three different diameters.

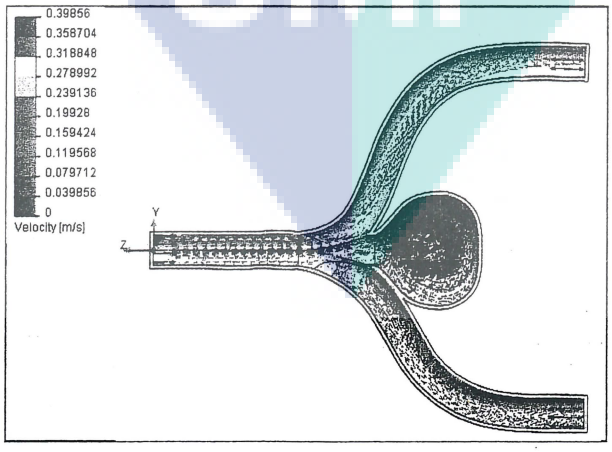

Figure 9: Velocity flow for radius 5mm

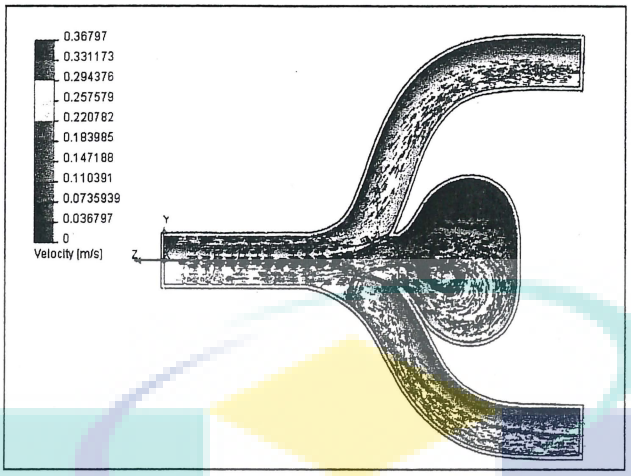

Figure 10: Velocity flow for radius 7mm

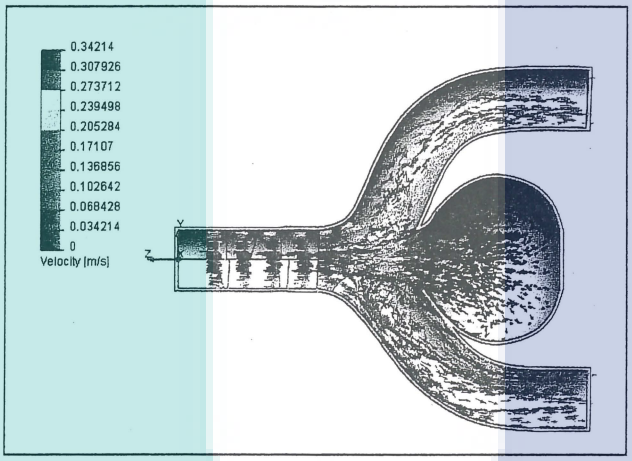

Figure 11: Velocity flow for radius 10mm

Flow Pattern of ruptured aneurysm

The pressure distribution pattern increase gradually for each stage due the expansion of aneurysm wall. This is apparently influence the increasing of pressure since the flow rate is constant. The obvious exchangeable pressure gradient at the aneurysm wall explained the deformation of the vortex at early proximal and late distal. Definitely, the presence of vortex is accelerates the aneurysm rupture as presented in figure 12 and 13. The pressure losses have an effect of aneurysm rupture which the blood takes a long time to pass through an aneurysm and energy losses is higher than unruptured aneurysm. Then, the energy losses transferred to energy of pressure and stress to load on the pathological aneurysm surfaces [21].

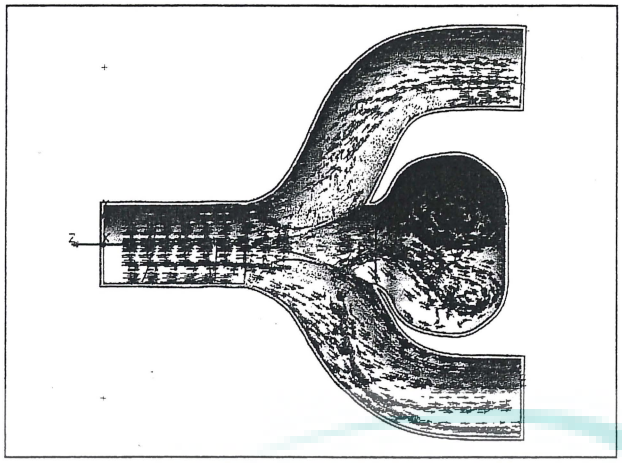

Figure 12: Velocity flow for radius 12mm

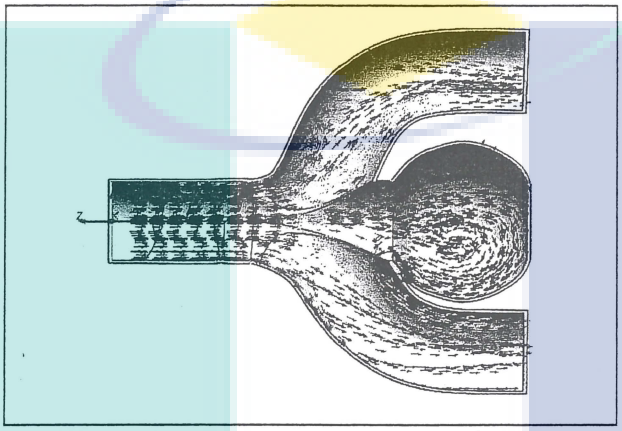

Figure 13: Velocity flow for diameter 14mm

Peak Velocity Correlation with diameter

Table 1: Peak velocity vs diameter

Diameter,mm	Peak velocity,m/s	
	Normal case	Abnormal case
5	0.3961	0.3937
7	0.3617	0.3385
10	0.3352	0.2836
12	0.3220	0.2397
14	0.3091	0.2041

Table 2: Peak velocity percentage vs diameter

Diameter,mm	Percentage peak velocity different,%
5	0.61
7	6.4
10	15.4
12	21.1
14	33.9

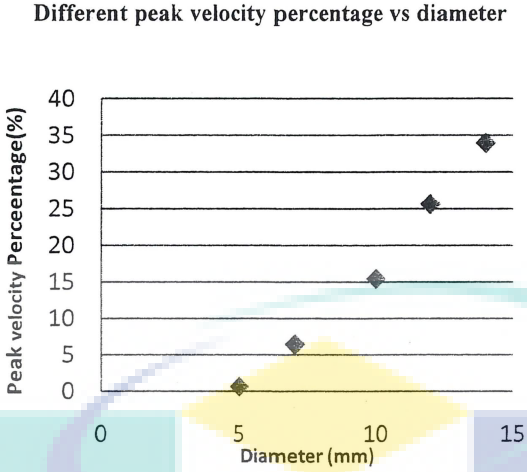

Figure 14: Graph percentage peak velocity different vs diameter

From the data shown in table 1, normal vessel and abnormal vessel have a different peak velocity. When increasing the diameter of the blood vessel, the peak pressure increase as well. Normal vessel have higher peak velocity than abnormal vessel. In general, bifurcation resulting the velocity of blood flow become lower even the vessel do not have any aneurysm in it. Flow pattern also effected by this phenomena at the bifurcation. The final correlation obtained show tabulated data in table 2 and figure 14 to describe precentage of peak velocity different on a variable diameter.

IV. CONCLUSION

The study establishes the correlation between diameter of the aneurysms and peak velocity for normal and abnormal case. This parameter represents the rupture prediction after the FSI approach apply to the problem described. For normal case, the lowest peak velocity is from the diameter of 5 mm. The highest peak pressure results from the largest diameter. As a consequence, the different percentage of peak velocity between normal and abnormal velocity proved that the aneurysm give an effect to the blood flow at the branches. The aneurysm effect can be seen from the velocity profile for different diameter of aneurysms. The smallest percentage is at 5mm with 0.61% and the largest is for diameter 14mm with 33.9%.

For future works, there is necessary improvement in the accuracy of the computational models in order to establish more reliable patient –specific index of aneurysms rupture.

REFERENCES

[1] Burt, H.M. & Hunter, W.L. (2006) "Drug-eluting stents: A multidisciplinary success story", *Advanced Drug Delivery Reviews*, vol. 58, pp. 350– 357.

[2] Borovetz, H.S., Burke, J.F. & Chang, T.M.S. (2004) "Application of materials in medicine, biology and artificial organs", in: B.D. Ratner, A.S. Hoffman, F.J. Schoen, J.E. Lemons (Eds.), *Biomaterials Science, 2nd edition*, Elsevier Academic Press, Boston, pp. 455–479.

[3] L.-D. Jou, "Effect of stent on flow in fusiform aneurysms", *Summer Bioengineering Conference*, June 25-29, (2003)

[4] Wilms, G. et al. 2002, "Endovascular Treatment of a Ruptured Paraclinoid Aneurysm of the Carotid Siphon Achieved Using Endovascular Stent and Endovascular Coil Placement," *American Journal of Neuroradiology*, Vol. 21, pp. 753-6.

[5] Brassel, E. et al. 2001, "Intravascular Stent Placement for a Fusiform Aneurysm of the Posterior Cerebral Artery: Case Report," *European Radiology*, Vol. 11, pp. 1250-3.

[6] Hatakeyama T, Shigematsu H, Muto T. Risk factors for rupture of abdominal aortic aneurysms based on three-dimensional study. J Vasc Surg 2001;33(3):453–61.

[7] Stringfellow MM, Lawrence PF, Stringfellow RG. The influence of aorta-aneurysm geometry upon stress in the aneurysm wall. J SurgRes 1987;42(4):425–33.

[8] Inzoli F, Boschetti F, Zappa M, Longo T, Fumero R. Biomechanical factors in abdominal aortic aneurysm rupture. Eur J Vasc Surg 1993;7(6):667–74
[9] Fillinger MF, Raghavan ML, Marra SP, Cronenwett JL, Kennedy FE. In vivo analysis of mechanical wall stress and abdominal aortic aneurysm rupture risk. J Vasc Surg 2002;36(3):589–97.
[10] Wang DHJ, Makaroun MS, Webster MW, Vorp DA. Effect of intraluminal thrombus on wall stress in patient-specific models of abdominal aortic aneurysm. J Vasc Surg 2002;36(3):598–604.
[11] Venkatasubramaniam AK, Fagan MJ, Mehta T, Mylankal KJ, Ray B, Kuhan G, et al. A comparative study of aortic wall stress using finite element analysis for ruptured and non-ruptured abdominal aortic aneurysms. Eur J Vasc Endovasc Surg 2004;28(2):168– 76
[12] Aenis, M., Stancampiano, A.P., Wakhloo, A.K. & Lieber,B.B. (1997) Modeling of flow in a straight stented and nonstented side wall aneurism model, *ASME Journal of Biomechanical Engineering,* vol. 119, pp. 206–212
[13] K. Perktold, R. Peter and M. Resch, "Pulsatile non-Newtonian blood flow simulation through a bifurcation with an aneurysm". *Biorheology*, 26: 1011-1030, 1989.
[14] C.J. Egelhoff, R.S. Budwig, D.F. Elger, T.A. Khraishi, K.H. Johansen, "Model studies of the flow in abdominal aortic aneurysms during resting and exercise conditions", *J. Biomech.* 32 (1999) 1319–1329.
[15] C.L. Asbury, J.W. Rwberti, E.I. Bluth, R.A. Peattie, "Experimental investigation of steady flow in rigid models of abdominal aortic aneurysm", *Ann. Biomed. Eng.* 23 (1995) 29–39.
[16] R.A. Peattie, T.J. Riehle, E.I. Bluth, "Pulsatile flow in fusiform models of abdominal aortic aneurysms: Flow fields, velocity patterns and flow-induced wall stresses", *ASME J. Biomech. Eng.* 126 (2004) 438–446.
[17] R. Balossino et al. "Effects of different stent designs on local hemodynamics in stented arteries, Journal of Biomechanics" 41 (2008) 1053–1061
[18] Miki Hirabayashi et al, "A lattice Boltzmann study of blood flow in stented aneurism", *Future Generation Computer Systems*, Elsevier B.V, 20 (2004) 925–934
[19] Gyorgy Paa´l a, A´ da´m Ugron a, Istva´n Szikora , Imre Bojta´r , "Flow in simplified and real models of intracranial aneurysms", *International Journal of Heat and Fluid Flow*. Elsevier B.V 28 (2007) 653–664
[20] Khalil M. Khanafer a, Prateek Gadhoke a, Ramon Berguer a,b and Joseph L. Bull a. Modeling pulsatile flow in aortic aneurysms: Effect of non-Newtonian properties of blood. Biorheology 43 (2006) 661–679
[21]Yi Qian, Tetsuji Harada, Koichi Fukui, Mitsuo Umezu, Hiroyuki Takao, and Yuichi Murayama. Hemodynamic Analysis of Cerebral Aneurysm and Stenosed Carotid Bifurcation Using CFD Technique. LSMS 2007, LNBI 4689, pp. 292–299, 2007.

CHAPTER 3

2nd technical paper published

4th International Conference on Advanced Computational Engineering and Experimenting, ACE-X 2010, 8& 9 July 2010, Paris, France

Biomechanical Modeling of Aneurysm Growth and Rupture using Fluid Structure Interaction

*M.Mazwan Mahat[1], A.Juliawati[2] and Ishkrizat Taib[3]

[1]University of Technology MARA, Shah Alam,, 40450 Shah Alam, Malaysia.

[2]Universiti Malaysia Pahang, Lebuhraya Tun Razak, 26300 Gambang, Malaysia.

[3]Universiti Tun Hussien Onn Malaysia, 86400 Parit Raja Batu Pahat, Malaysia.

*Corresponding author: mazwan@salam.uitm.edu.my

Tel:+603-55436248

Abstract

We develop a method to analyze aneurysm growth and rupture based on idealized spherical shape from actual patient specific geometry data. This study purposely carried out to evaluate whether wall mechanics of soft tissue coupled with blood flow dynamics can be used to provide the insight weakening phenomena. In order to simulate the behavior of the system, the fluid structure interaction method (FSI) was utilized using transferred data from fluid dynamics model to finite element wall mechanics. The FSI transferred these dynamics loads to exert the aneurysms wall then the respective deformations determined. The numerical modeling of aneurysms results the blood flow parameter of pressure and velocity inside aneurysm sac in the form of profile correlations. These parameters generate a possible aneurysms ruptures timing during the growth as a reasonable quantitative observations. The developed method allows us to identify biomechanical factors that can influence the blood flow properties changes and wall stress distribution. As part of the computed maximum wall stress to relate with growth and rupture, normalized velocity and pressure profiles inside the aneurysm sac were correlated. This explains the effect of blood flow to the weakening vessel wall and rupture behaviour due to variable flow conditions. These results assist medical practitioner to the prediction of time and location of aneurysm ruptured.

Keywords: *Abdominal Aortic Aneurysm, Numerical method, Fluid structure interaction.*

1. INTRODUCTION

Abdominal aortic aneurysm is a bulging and widening of the blood vessel due the weakening of aortic wall which may prone to rupture of aneurysm. Normally, in clinical practice, surgical treatment of AAA is considered after the maximal diameter exceeds 5-6 cm [1]. Nevertheless, the increasing of the aneurysm region may eventually increase the risk of rupture [2] although, rupture could occur in a small aneurysm [1]. To study deeper in detection of aneurysm rupture, both of non-geometric patient characteristic and geometric properties should be considered [3] In recent study, computational model of mechanical behaviour in AAA is most prominent trend in AAA rupture risk assessment through the improvement of imaging and segmentation [4].

Study on idealised geometries model shown the wall stress is significantly reduced in presence of intraluminal thrombus (ILT) but the size of aneurysm and constitutive properties of aortic wall is considered [5]. In addition, the effect of aneurysm wall was increasing due the presence of atherosclerotic plaques inside blood vessel [5]. Furthermore, the stress distribution was depended on the real AAA shapes as well as the maximum diameter [4]. There is a highly complex of AAA in vivo shape and far from axisymmetric [10], which specific wall stress assessment and finite element models were the mainly approach need to be based on detailed for AAA geometry of those three dimensional description. The complex wall stress distribution was shown from the modeled based on patient-specific geometries [6], which may influence after the presence of ILT [7]. Furthermore, there has been related between the occurrence and location [8] of aneurysm rupture and the peak wall stress value that computed from this aneurysm model. From the observation, the peak wall stress was a better predictor of aneurysm rupture than diameter in AAA [6]. The boundary condition for the pressure load was applied at the aortic wall which is resulted from the coupled of blood velocity and pressure

Besides that, the method of generating patient-mesh for specific hexahedral finite element on AAA lumen and wall is represented to facilitate the incorporating fluid/structure interaction for assessment of AAA wall stress. This incorporating should be illustrated by simulation in AAA characteristic.

2. NUMERICAL MODELING

In this study, fluid structure interaction analysis (FSI) is used to model the effect of blood flow to the weakening aorta wall. Sequential usages of commercially available numerical modelling software were used to determine the flow structure and the behaviour of the aorta wall during aneurysm. Data were exchanged between the models and analysis was done to determine the behaviour.

The aneurysm was simplified in a three-dimensional model which was constructed using Engineering Fluid Dynamic (EFD) software. The thickness of the blood vessel was set to 1.5mm throughout, and was gradually reduced after the expansion of the aneurysm region. The idealized model of a blood vessel with cylindrical symmetry has been commonly used in haemodynamic studies because the deviations within a segment of nondiseased blood vessel are too small to significantly alter the flow field. The geometry of the diseased region is normally not symmetrical, but in the present study cylindrical symmetry is assumed.

The viscosity of blood was assumed to be constant because changes in viscosity is relatively small for vessel diameter larger than 0.5mm [10]. This study also focused on the basic flow dynamics, so Newtonian behaviour is sufficient for approximation purpose [12]. For simplicity, the flow is considered to be incompressible, homogeneous and non-pulsatile.

Gravitational force was ignored and the cavity was assumed to be filled with stagnant blood, i.e. no endoleaks are assumed in stented aneurysm models.

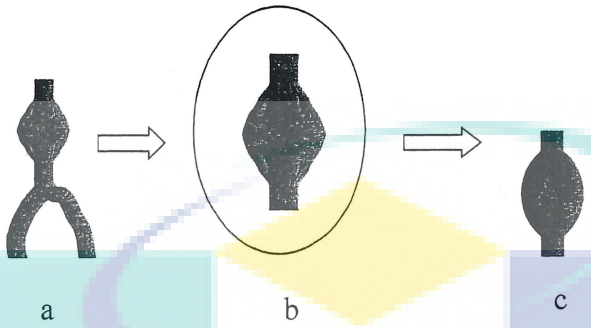

Figure 1: Abdominal Aortic Aneurysm (a) real aneurysm (b) aneurysm side (c) simplified aneurysm model.

In this study, Navier-Stokes equations, which are formulations of mass, momentum and energy conservation laws for fluid flows were solved. The equations are supplemented by fluid state equations defining the nature of the fluid, and by empirical dependencies of fluid viscosity and/or thermal conductivity on temperature. A particular problem is finally specified by the definition of its geometry, boundary and initial conditions. The mass, momentum and energy conservation laws in a Cartesian coordinate system rotating at the Ω angular velocity about an axis passing through the coordinate system's origin can be written in the conservation form as follows:

$$\frac{\partial \rho}{\partial t} + \frac{\partial}{\partial x\kappa}(\rho u\kappa) = 0 \qquad (1)$$

$$\frac{\partial \rho ui}{\partial t} + \frac{\partial}{\partial x\kappa}(\rho ui.uik) + \frac{\partial P}{\partial xi} = Si \qquad (2)$$

$$\frac{\partial(\rho \mathrm{E})}{\partial t}+\frac{\partial}{\partial x \kappa}((\rho \mathrm{E}+P) \mathcal{U} \kappa+q \kappa-\tau i k \mathcal{U} i \quad (3)$$

where u is the fluid velocity, ρis the fluid density, is a mass-distributed external force per unit mass due to a porous media resistance (Si*porous*), a buoyancy (Si*gravity*), and the coordinate system's rotation (Si*rotation*), i.e., Si = Si*porous* + Si*gravity* + Si*rotation*, E is the total energy per unit mass, Q_H is a heat source per unit volume, τ_{ik} is the viscous shear stress tensor, q_i is the diffusive heat flux, and the subscripts are an expression to denote summation over the three coordinate directions.

$$\tau_{ij}^{\mathcal{R}}=\mu_t\left(\frac{\partial u_i}{\partial x_j}+\frac{\partial u_j}{\partial u_i}+\frac{2}{3}\frac{\partial u_j}{\partial x_i}\mathcal{S}_{ij}\right)-\frac{2}{3}\rho k\mathcal{S}_{ij} \quad (4)$$

For Newtonian fluids the viscous shear stress tensor is defined as

$$\tau_{ij}=\mu\left(\frac{\partial u_i}{\partial x_j}+\frac{\partial u_j}{\partial u_i}+\frac{2}{3}\frac{\partial u_j}{\partial x_i}\mathcal{S}_{ij}\right)-\frac{2}{3}\rho k\mathcal{S}_{ij} \quad (5)$$

Where

$$\mu=\mu_l+\mu_t \quad (6)$$

Here $\mathcal{S}_{ij}$ is the Kronecker delta function (it is equal to unity when $i = j$, and zero otherwise),μ_l is the dynamic viscosity coefficient, μ_t is the turbulent eddy viscosity coefficient and k is the turbulent kinetic energy. Note that μ_t and k are zero for laminar flows. In the frame of the ***k-ε***turbulence model, μ_t is defined using two basic turbulence properties, namely, the turbulent kinetic energy ***k*** and the turbulent dissipation ε,

$$\mu_t=f_\mu\frac{C_\mu\rho k^2}{\epsilon} \quad (7)$$

Here, f_μ is a turbulent viscosity factor. It is defined by the expression

$$f_\mu=\left[1-exp(-0.025R_y)\right]^2.\left(1+\frac{20.5}{R_T}\right) \quad (8)$$

Where,

$$R_T=\frac{\rho k^2}{\mu_l\varepsilon}, R_y=\frac{\rho\sqrt{ky}}{\mu_l} \quad (9)$$

and y is the distance from the wall. This function allows us to take into account laminar-turbulent transition.

Two additional transport equations are used to describe the turbulent kinetic energy and dissipation,

$$\frac{\partial \rho k}{\partial t} + \frac{\partial}{\partial x_k}(\rho u_k k) = \frac{\partial}{\partial x_k}\left(\left(\mu_l + \frac{\mu_t}{\sigma_k}\right)\frac{\partial k}{\partial x_k}\right) + S_k \qquad (10)$$

$$\frac{\partial \rho \varepsilon}{\partial t} + \frac{\partial}{\partial x_k}(\rho u_k \varepsilon) = \frac{\partial}{\partial x_k}\left(\left(\mu_l + \frac{\mu_t}{\sigma_\varepsilon}\right)\frac{\partial \varepsilon}{\partial x_k}\right) + S_\varepsilon \qquad (11)$$

Here P_B represents the turbulent generation due to buoyancy forces and can be written as

$$P_B = -\frac{g_i}{\sigma_B}\frac{1}{\rho}\frac{\partial \rho}{\partial x_i} \qquad (12)$$

where g_i is the component of gravitational acceleration in direction x_i, the constant σ_B= 0.9, and constant is defined as: C_B = 1when , and C_B = 0 otherwise;

$$f1 = 1 + \left(\frac{0.05}{f_\mu}\right)^3, f2 = 1 - exp(-R_T^2) \qquad (13)$$

The constants Cμ, $C\varepsilon_1$, Cε2 ,σk , σε are defined empirically. In that software, the following typical values are used:

$$C_\mu = 0.09, C_{\varepsilon l} = 1.44, C_{\varepsilon 2} = 1.92, \sigma_\varepsilon = 1.3$$

$$\sigma_k = 1$$

These equations describe both laminar and turbulent flows. Moreover, transitions from one case to another and back are possible. The parameters k and μ_t are zero for purely laminar flows.

3. RESULTS AND DISCUSSIONS

3.1 Velocity behavior

Figure 2 shows the profile for *x*-velocity along the centerline perpendicular to the inlet flow in the aneurysm. The results agree with that of Khanafer et al (2006). It is observed that a very weak recirculation or vortex is present at the distal area. This is the sign that implies energy loses inside the aneurysm. The energy loses may be transferred to the energy of pressure and stress to load on pathological aneurysm surface which the surface frequently shrunk and drawn [9]. Khanafer (2006) expected that the speed decreases as a blood travels from proximal to distal end due the increase of aneurysm diameter, inline with the basic flow theory. The negative values in the profile depict the reverse flow of blood travel in distal end. The velocity behavior for each stage of aneurysm is illustrated further more in Figure 3. For this results, different diameter of aneurysm was used in order to suit other related study. From Figure 3, where *x*-velocity profiles are compiled for three different stages near the proximal area, it can be seen that no vortex can be detected for all three stages. posess the same pattern of flow with reduced values as the aneurysm grows. This phenomenon is in line with the continuity equation that, when the dilation area expands, the velocity reduces since the flow rate is constant. The unstable flow occurred in aneurysm produce vortex deformation. The curvature gradient in x-velocity component at distal neck depicted the strong formation of vortex. The vortex occurred in aneurysm contributed the energy losses of the fluid and unable to recover after the flow entering back to the normal artery. In summary, due the increment of diameter in aneurysm, the blood velocity will experience some deduction. This will apparently increase the pressure since the flow rate is constant.

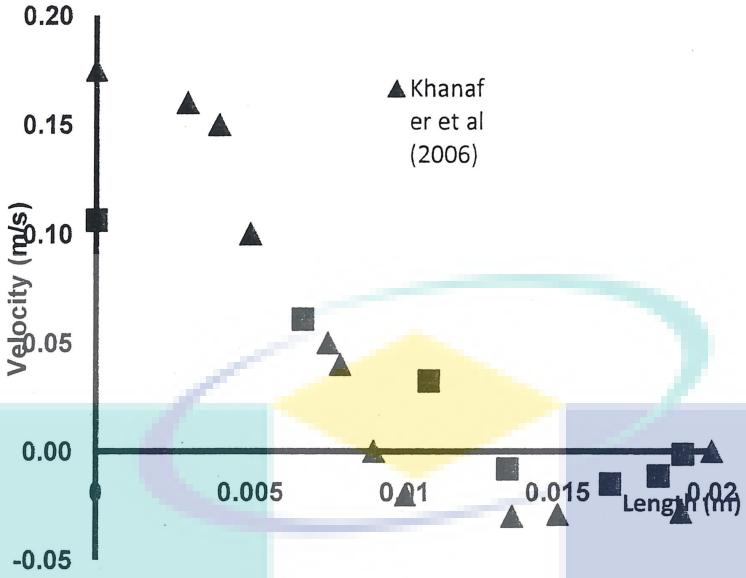

Figure 2: The *x*-velocity profile for the centerline perpendicular to the inlet flow.

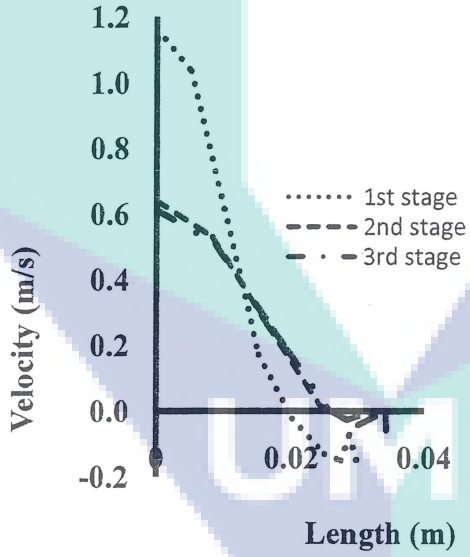

Figure 3: The *x*-velocity profile along the centerline, perpendicular to the inlet flow.

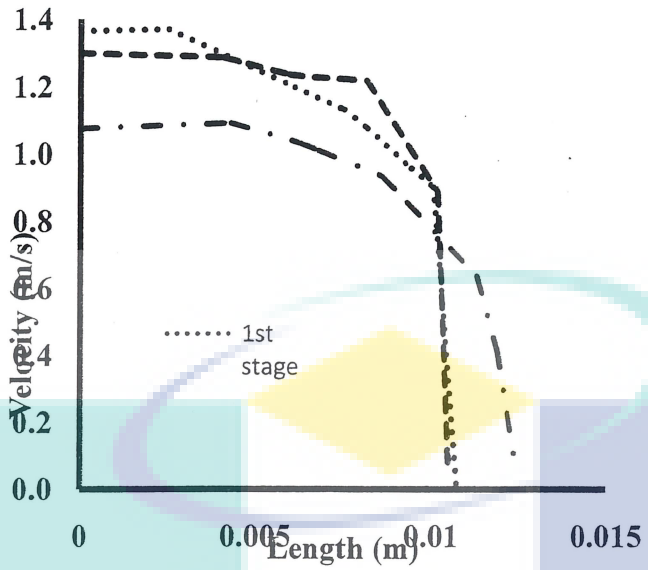

Figure 4: velocity profile at the distal in cross sectional of aneurysm

3.2 Pressure distribution

Pressure gradient is affected the deformation of the aneurysm wall in a certain time period until ruptured if not surgically treated. The correlation between the peak pressure and aneurysm deformation are investigate to prove that the increment of the aneurysm wall occurred due the pressure raise. Figure 2 is illustrated development of aneurysm from the early of aneurysm detection by CT scan until it assumed be ruptured. There are 3 stages of aneurysm deformation shows in a curvature. The pressure distribution pattern increase gradually for each stage due the expansion of aneurysm wall. This is apparently influence the increasing of pressure since the flow rate is constant. The obvious exchangeable pressure gradient at the aneurysm wall explained the deformation of the vortex at early proximal and late distal. Definitely, the presence of vortex is accelerates the aneurysm rupture. The pressure losses have an effect of aneurysm rupture which the blood takes a long time to pass through an aneurysm and energy losses is higher than unruptured aneurysm. Then, the energy losses transferred to energy of pressure and stress to load on the pathological aneurysm

surfaces [9](Yi Qian1). The polynomial curvature has interpret the correlation between peak pressure and each stage of aneurysm deformable (refer figure 5) which is the pressure rise proportional with the increment of dilation area. The obvious curvature discrepancy between 2nd stage and 3rd stage explained the higher pressure been applied at 3rd stage where if the pressure increase, the rupture risk become high. The aneurysm growth can be explained in millimeter (refer figure 6) where the 1st stage is considered as a reference. Previous study stated that the clinical diagnose the high expansion rate is 0.5 cm per year and up. The recirculation flow inside the aneurysm is related a dilation of aneurysm growth proportional the reduction of the wall thickness. The obvious increment from 2nd stage to 3rd stage (from 3.823mm to 5.847) predicted the strong vortex occurred inside the aneurysm. Then, the steeply increase of the aneurysm growth is predicted the ruptured can be occurred at the aneurysm wall.

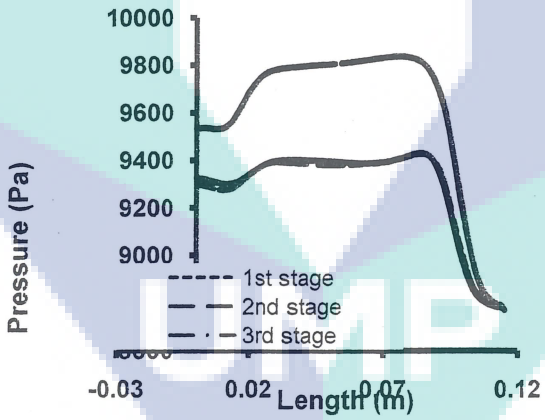

Figure 5: Pressure distribution along the aneurysm wall.

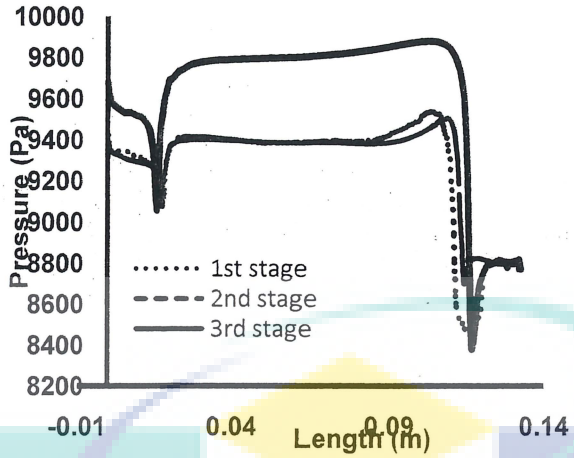

Figure 6: Pressure distribution along the centerline of aneurysm.

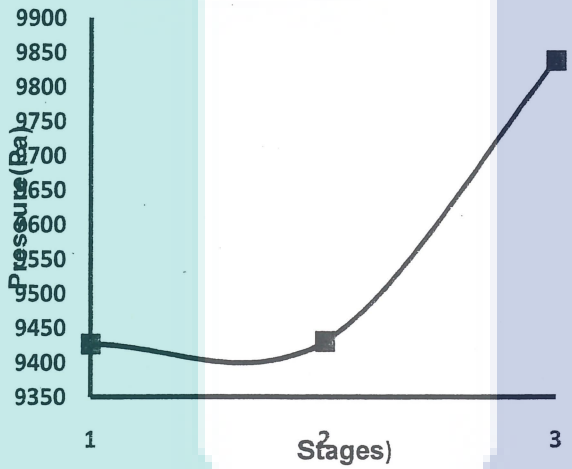

Figure 7: Correlation between peak pressure and each stages of aneurysm deformable.

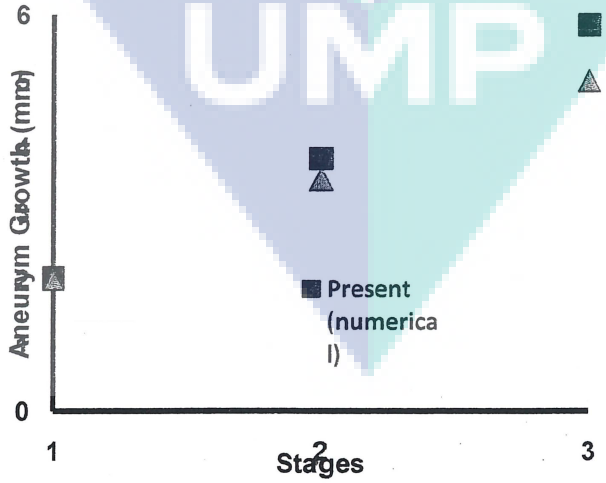

Figure 8: The percentages of aneurysm growth for each stage of aneurysm deformable.

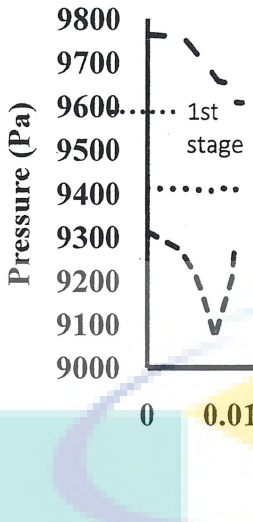

Figure 9: Pressure distribution at the proximal in cross sectional of aneurysm.

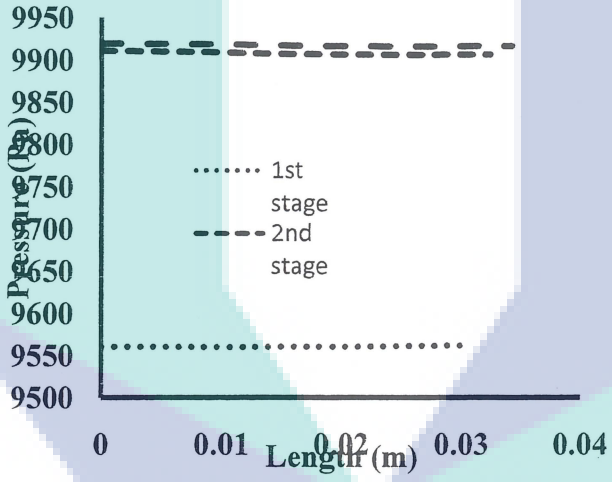

Figure 10: Pressure distribution at the middle in cross sectional of aneurysm.

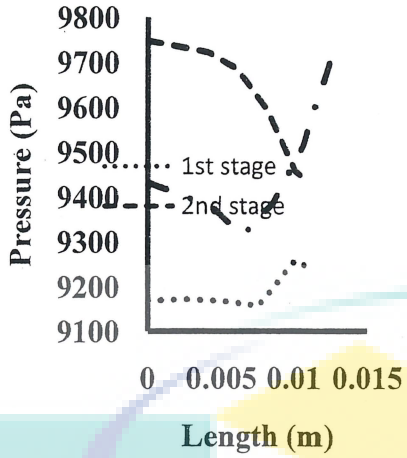

Figure 11: Pressure distribution at the distal in cross sectional of aneurysm.

3.3 Fluid shear stress distribution

Figure 5 is illustrated the shear stress profile between blood and aneurysm wall. The oscillatory curvature from proximal to distal neck explained the unstable flow occurred. The unstable flow is predicted as a vortex deformation inside the aneurysm. In early proximal, the deformation of vortex was detected. The deformation of vortex influences the energy losses inside the aneurysm. At the late distal, the strong deformation of vortex is expected occurred inside the aneurysm because of the immediate increment of curvature shows in figure 7. The vortex deformation increase the rate of aneurysm ruptured. The recirculation flow and vortex deformation near the aneurysm wall would produce the oscillatory curvature along the aneurysm region. The shear stress pattern was validated by Khanafer (2006) curvature which shows a similar pattern with the present study

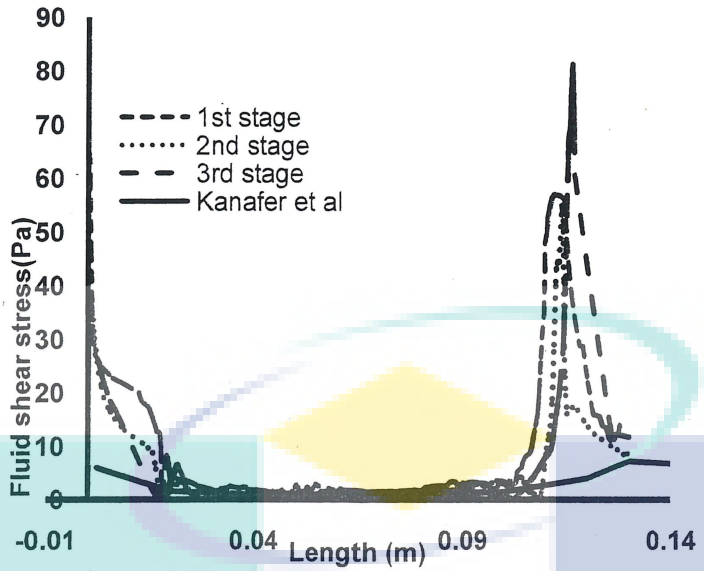

Figure 12: Shear stress distribution along the aneurysm region

4. CONCLUSION

In this study, there are several limitation should be issues. The AAA was simplified and underlying assumption in a presence study. The rigid wall model was assumed in hemodynamic pressure field. Previous study shown both of experimentally and computational which arterial wall model have a minor quantitative effect on computed a shear stress wall whereas the flow feature are preserved.

There is necessary the improvement in the accuracy of the computational models in order to establish more reliable patient –specific index of AAA rupture. Hence, the realistic boundary condition extracted from patient in vivo to computational is requires to impose that extracted model involve the couple of solid dynamic and fluid. The result demonstrates that when the pressure is applied on the wall, a degree of under prediction in computed AAA occurred. However, this study has a limitation for the clinical study but it's still used for the future study especially in fluid flow and fluid structure interaction due to establish the degree of error associated with the simplified model in decoupled approach. Finally, this study is

present the flow pattern in blood vessel through the modelling of the actual expanded that had designed in three dimension.

ACKNOWLEDGEMENT

The support-of the University of Technology Malaysia, under the Computatonal Fluid Mechanics and Computational Solid Mechanics Laboratory is gratefully acknowledged.

REFERENCES

[1] Lederle FA, Wilson SE, Johnson GR, Reinke DB, Littooy FN, Acher CW, et al. Immediate repair compared with surveillance of small abdominal aortic aneurysms. N Engl J Med 2002;346(19):1437–44

[2] Szilagyi DE, Elliott JP, Smith RF. Clinical fate of the patient with asymptomatic abdominal aortic aneurysm and unfit for surgical treatment. Arch Surg 1972;104(4):600–6.

[3] Hatakeyama T, Shigematsu H, Muto T. Risk factors for rupture of abdominal aortic aneurysms based on three-dimensional study. J Vasc Surg 2001;33(3):453–61.

[4] Stringfellow MM, Lawrence PF, Stringfellow RG. The influence of aorta-aneurysm geometry upon stress in the aneurysm wall. J SurgRes 1987;42(4):425–33.

[5] Inzoli F, Boschetti F, Zappa M, Longo T, Fumero R. Biomechanical factors in abdominal aortic aneurysm rupture. Eur J Vasc Surg 1993;7(6):667–74.

[6] Fillinger MF, Raghavan ML, Marra SP, Cronenwett JL, Kennedy FE. In vivo analysis of mechanical wall stress and abdominal aortic aneurysm rupture risk. J Vasc Surg 2002;36(3):589–97.

[7] Wang DHJ, Makaroun MS, Webster MW, Vorp DA. Effect of intraluminal thrombus on wall stress in patient-specific models of abdominal aortic aneurysm. J Vasc Surg 2002;36(3):598–604.

[8] Venkatasubramaniam AK, Fagan MJ, Mehta T, Mylankal KJ, Ray B, Kuhan G, et al. A comparative study of aortic wall stress using finite element analysis for ruptured and non-ruptured abdominal aortic aneurysms. Eur J Vasc Endovasc Surg 2004;28(2):168–76.

[9] Yi Qian, Tetsuji Harada, Koichi Fukui, Mitsuo Umezu, Hiroyuki Takao, and Yuichi Murayama3 Hemodynamic Analysis of Cerebral Aneurysm and Stenosed Carotid Bifurcation Using Computational Fluid Dynamics Technique. LSMS 2007, LNBI 4689, pp. 292–299, 2007.

[10] Aenis, M., Stancampiano, A.P., Wakhloo, A.K. & Lieber,B.B. (1997) Modeling of flow in a straight stented and nonstented side wall aneurism model, *ASME Journal of Biomechanical Engineering,* vol. 119, pp. 206–212.

[11] Khalil M. Khanafer a, Prateek Gadhoke a, Ramon Berguer a,b and Joseph L. Bull a. Modeling pulsatile flow in aortic aneurysms: Effect of non-Newtonian properties of blood. Biorheology 43 (2006) 661–679

CONCLUSIONS AND RECOMMENDATIONS

Conclusions

The study establishes the correlation between diameter of the aneurysms and peak velocity for normal and abnormal case. This parameter represents the rupture prediction after the FSI approach apply to the problem described. For normal case, the lowest peak velocity is from the diameter of 5 mm. The highest peak pressure results from the largest diameter. As a consequence, the different percentage of peak velocity between normal and abnormal velocity proved that the aneurysm give an effect to the blood flow at the branches. The aneurysm effect can be seen from the velocity profile for different diameter of aneurysms. The smallest percentage is at 5mm with 0.61% and the largest is for diameter 14mm with 33.9%. Furthermore, when the pressure is applied on the wall, a degree of under prediction in computed AAA occurred. However, this study has a limitation for the clinical study but it's still used for the future study especially in fluid flow and fluid structure interaction due to establish the degree of error associated with the simplified model in decoupled approach.

Recommendations

1. Use more accurate computational model.
2. Use specific index of aneurysm ruptured.
3. Use the real boundary condition extracted from patient to impose the extracted model.

References

[1] Dumoulin, C. & Cochelin, B. (2000) Mechanical behavior modelling of balloon-expandable stents, *Journal of Biomechanics,* vol. 33, pp. 1461–1470.

[2] Petrini, L., Migliavacca, F., Auricchio, F. & Dubini, G. (2004) Numerical investigation of the intravascular coronary stent flexibility, *Journal of Biomechanics,* vol. 37, pp. 495–501.

[3] Rogers, C., Tseng, D.Y., Squire, J.C. & Edelman, E.R. (1999) Balloon– artery interactions during stent placement. A finite element analysis approach to pressure, compliance, and stent design as contributors to vascular injury, *Circulation Research,* vol. 84, pp. 378-383.

[4] Lally, C., Dolan, F. & Prendergast, P.J. (2005) Cardiovascular stent design and vessel stresses: a finite element analysis, *Journal of Biomechanics*, vol. 38, pp. 1574– 1581

[5] Lieber, B. B. et al., 2002, "The Physics of Endoluminal Stenting in the Treatment of Cerebrovascular Aneurysms", *Annals of Biomedical Engineering*, Vol. 30, pp. 768-777.

[6] Miki Hirabayashi et al, "A lattice Boltzmann study of blood flow in stented aneurism", *Future Generation Computer Systems*, Elsevier B.V, 20 (2004) 925–934